Wavelet-Based Estimation of the Nonstationary Mean Signal in Wireless Systems

Ravi Narasimhan, *Member, IEEE,* and Donald C. Cox, *Fellow, IEEE*

***Abstract*—A new technique is described for estimating the nonstationary mean signal received at a mobile station in a Rayleigh fading environment. The estimate is based on samples taken at the midpoints between the local minima of the received envelope. The continuous wavelet transform is used to estimate the local minima. An estimate of the mean signal is obtained using a fixed number of local minima. This technique requires neither an estimate of the mobile speed nor an adaptive temporal averaging window, in contrast to other estimators. Simulations show that the mean signal is estimated well in a nonstationary environment with variable mobile speed.**

***Index Terms*—Nonstationary signal analysis, wavelets, wireless communication.**

I. Introduction

A SIGNIFICANT characteristic of wireless systems is the signal variation caused by the movement of the mobile stations. An estimate of the local mean of the received signal is useful to determine the quality of a radio link. The mean signal is also needed in handoff, power control, and channel assignment algorithms. Accurate estimates of the mean signal improve the performance of system control algorithms and thereby increase the realized system capacity.

In many environments, a direct path is not present between the base station and the mobile station. The received signal consists of a sum of waves which have been reflected by objects such as mountains, trees, and buildings. The sum of many waves at the receiver gives rise to small-scale spatial variation of the received envelope (on the order of a wavelength). In situations where there is no dominant path between the base station and the mobile station, the small-scale spatial variation is called Rayleigh fading [1]. The received signal is nonstationary for distances on the order of building sizes since the mean of the small-scale variation changes considerably. This large-scale variation of the mean is known as shadowing. The mean of the shadowing also decreases as the distance between the base station and the mobile station increases.

The mean signal is the local mean of the small-scale variation (up to a constant) and represents the distance-dependent trend and shadowing. The most widely used estimate of the mean signal is the average of samples of the received envelope (or logarithm of the envelope) taken at a constant temporal interval. In [2], the bandwidth of a continuous-time lowpass filter is chosen to minimize the estimation error for a nominal constant mobile speed. Reference [3] estimates the mean signal by a spatial analog averaging filter and determines the number of uncorrelated samples needed for discrete-time averaging under the assumption that signal samples taken at constant spatial intervals are available. Another paper [4] derives the minimum-variance unbiased estimator for the mean signal in a Rayleigh fading environment under the assumption that all samples used in the estimate have the same mean and are uncorrelated. Since in [4] the samples must be taken at a constant temporal interval, the assumption places constraints on the unknown and possibly time-varying mobile speed. An adaptive method to estimate the mean signal for Rayleigh fading is proposed in [5] where the squared deviations of the logarithm of the received envelope are used to estimate the maximum Doppler frequency. The maximum Doppler frequency is then used to adapt the number of signal samples that are averaged to estimate the mean signal. The papers mentioned above have considered only the problem of a constant, possibly unknown, mobile speed. For variable mobile speeds, the number of temporal signal samples used in the estimate of the mean signal must be constantly adapted, and the rate of adaptation is critical to the performance of the estimator. In particular, errors in the estimate of the maximum Doppler frequency as described in [5] could magnify errors in the estimate of the mean signal due to suboptimal temporal averaging windows.

A new method of estimating the mean signal using wavelets is described in this paper. The wavelet transform at different scales corresponds to a variety of window lengths and hence eliminates the necessity of adapting the duration of a single temporal averaging window. The method presented here utilizes the fact that the small-scale spatial variation of the received envelope is dominated by the positions of the mobile and base stations. This spatial variation has a characteristic scale that is on the order of a carrier wavelength. By averaging over a fixed number of samples taken at the midpoints between the local minima of the received envelope, one can obtain an estimate of the mean signal over a spatial scale that is selected based on the variation of the distance-dependent trend and shadowing.

The paper is organized as follows. In Section II, wireless propagation and noise models are presented. Section III presents a method to estimate the local minima of the received envelope using the continuous wavelet transform (CWT). Signal samples taken at the midpoints between the local minima are then used to estimate the mean signal. Section IV addresses the selection of parameters used in the estimate of the mean signal and compares the performance with the adaptive averaging method of [5] for constant and variable mobile speed. Conclusions are given in Section V.

Manuscript received February 24, 2000; revised June 20, 2000. This work was supported by a National Science Foundation Graduate Research Fellowship.

R. Narasimhan is with Marvell Semiconductor, Inc., Sunnyvale, CA 94085 USA (e-mail: nkravi@wireless.stanford.edu).

D. C. Cox is with the Department of Electrical Engineering, Stanford University, Stanford, CA 94305-9515 USA (e-mail: dcox@spark.stanford.edu).

Publisher Item Identifier S 0733-8716(00)09213-1.

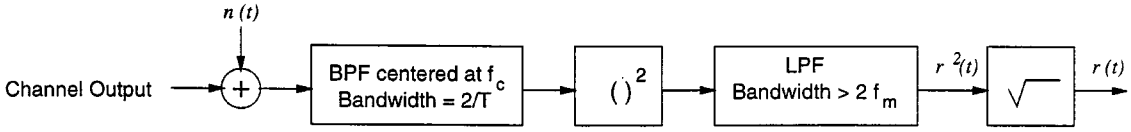

Fig. 1. Receiver model for recovering signal envelope.

II. Wireless Propagation and Noise Models

The propagation model discussed here takes into account three effects which are present in many wireless environments: correlated Rayleigh fading, correlated log-normal shadowing, and a distance-dependent trend [1]. The received bandpass signal at a mobile consists of a sum of contributions from several paths. Let $r_c(\boldsymbol{x})$ denote the complex envelope of the received signal at position $\boldsymbol{x}$. For a large number of multipath components, $r_c(\boldsymbol{x})$ is an approximate wide-sense stationary complex Gaussian process in a small neighborhood of $\boldsymbol{x}$. Let $s(\theta)$ denote the distribution of incoming power in angle θ in a plane with respect to the mobile velocity. We denote $p(\boldsymbol{x}, \boldsymbol{x_B})$ to be the received power at the mobile station averaged over a small neighborhood of $\boldsymbol{x}$ due to a base station located at $\boldsymbol{x_B}$. Let λ represent the carrier wavelength. From the above conditions and for an omnidirectional antenna, the autocorrelation of $r_c(\boldsymbol{x})$ for a mobile velocity in the direction $\hat{\boldsymbol{u}}$ and for a small neighborhood of $\boldsymbol{x}$ can be written as

$$\begin{aligned} &A_{r_c r_c}(y, p(\boldsymbol{x}, \boldsymbol{x_B})) \\ &\quad = \tfrac{1}{2} E\{r_c(\boldsymbol{x} + y\hat{\boldsymbol{u}}) r_c^*(\boldsymbol{x})\} \\ &\quad = p(\boldsymbol{x}, \boldsymbol{x_B}) \int_{-\pi}^{\pi} e^{j(2\pi y \cos\theta/\lambda)} s(\theta)\, d\theta. \end{aligned} \tag{1}$$

The autocorrelation explicitly indicates the fact that $r_c(\boldsymbol{x})$ is wide-sense stationary only in a small neighborhood of $\boldsymbol{x}$. Let $\langle \boldsymbol{a}, \boldsymbol{b} \rangle$ denote the inner product between vectors $\boldsymbol{a}$ and $\boldsymbol{b}$. A model for $r_c(\boldsymbol{x})$ (for travel in the direction $\hat{\boldsymbol{u}}$) can be shown to be

$$\begin{aligned} r_c(\boldsymbol{x}) = &\left[\frac{4\pi p(\boldsymbol{x}, \boldsymbol{x_B})}{K}\right]^{1/2} \sum_{k=0}^{K-1} \sqrt{s(\theta_k)} \\ &\times \exp\left\{ j \left[\frac{2\pi \langle \boldsymbol{x}, \hat{\boldsymbol{u}} \rangle}{\lambda} \cos\theta_k + \phi_k(\boldsymbol{x}, \boldsymbol{x_B}) \right] \right\} \end{aligned} \tag{2}$$

where K is the number of terms in the model, $\theta_k = -\pi + 2\pi(k + 1/2)/K, k = 0, \ldots, K-1$, and $\phi_k(\boldsymbol{x}, \boldsymbol{x_B})$ are i.i.d. uniformly on $[-\pi, \pi)$. The autocorrelation of (2) approaches (1) as $K \to \infty$.

The average received power $p(\boldsymbol{x}, \boldsymbol{x_B})$ contains the distance-dependent trend and log-normal shadowing [6]. Let α represent the exponent of the distance-dependent trend. Furthermore, let $10^{L(\boldsymbol{x}, \boldsymbol{x_B})/10}$ denote the log-normal shadowing between the mobile position $\boldsymbol{x}$ and the base station position $\boldsymbol{x_B}$. The received power averaged over a neighborhood of $\boldsymbol{x}$ due to the base station located at $\boldsymbol{x_B}$ can then be expressed as

$$p(\boldsymbol{x}, \boldsymbol{x_B}) = P_0 \|\boldsymbol{x} - \boldsymbol{x_B}\|^{-\alpha} 10^{L(\boldsymbol{x}, \boldsymbol{x_B})/10} \tag{3}$$

where P_0 accounts for antenna parameters, transmitted power, and other relevant system parameters. The process $L(\boldsymbol{x}, \boldsymbol{x_B})$ is modeled as a zero-mean Gaussian random process which is wide-sense stationary in the variable $\boldsymbol{x}$. Let $A_{LL}(y, \boldsymbol{x_B})$ denote the autocorrelation of $L(\boldsymbol{x}, \boldsymbol{x_B})$ in the variable $\boldsymbol{x}$ along the direction $\hat{\boldsymbol{u}}$. An empirical model for $A_{LL}(y, \boldsymbol{x_B})$ is [7]

$$A_{LL}(y, \boldsymbol{x_B}) = \sigma_L^2(\boldsymbol{x_B}) \exp\left(-\frac{|y|}{d_0(\boldsymbol{x_B})} \right) \tag{4}$$

where $\sigma_L^2(\boldsymbol{x_B})$ and $d_0(\boldsymbol{x_B})$ are the variance and correlation length of $L(\boldsymbol{x}, \boldsymbol{x_B})$, respectively. The power spectrum $S_{LL}(\nu, \boldsymbol{x_B})$ of $L(\boldsymbol{x}, \boldsymbol{x_B})$ is given by

$$S_{LL}(\nu, \boldsymbol{x_B}) = \frac{2 d_0(\boldsymbol{x_B}) \sigma_L^2(\boldsymbol{x_B})}{1 + [2\pi\nu d_0(\boldsymbol{x_B})]^2} \tag{5}$$

where ν denotes spatial frequency. Let $\nu_{\max}$ denote the maximum spatial frequency of $S_{LL}(\nu, \boldsymbol{x_B})$ that is taken into account, and let $\tilde{D}$ be the distance traveled by the mobile within a time period of interest. We define $D = \max(\tilde{D}, I d_0)$ where $I \gg 1$. A model for the process $L(\boldsymbol{x}, \boldsymbol{x_B})$ can be shown to be

$$\begin{aligned} L(\boldsymbol{x}, \boldsymbol{x_B}) = &\sum_{k=-J}^{J-1} \left[\frac{2}{CD} S_{LL}\left(\frac{(k+1/2)}{D}, \boldsymbol{x_B} \right) \right]^{1/2} \\ &\times \cos\left[\frac{2\pi \langle \boldsymbol{x}, \hat{\boldsymbol{u}} \rangle}{D} (k + 1/2) + \beta_k(\boldsymbol{x}, \boldsymbol{x_B}) \right] \end{aligned} \tag{6}$$

where

$$\begin{aligned} C &= \frac{1}{D \sigma_L^2(\boldsymbol{x_B})} \sum_{k=-J}^{J-1} S_{LL}\left(\frac{(k+1/2)}{D}, \boldsymbol{x_B} \right) \\ \nu_{\max} &= J/D \end{aligned} \tag{7}$$

and $\beta_k(\boldsymbol{x}, \boldsymbol{x_B})$ are i.i.d. uniformly on $[-\pi, \pi)$. The received envelope $|r_c(\boldsymbol{x})|$ is Rayleigh distributed in the absence of noise.

The noise model developed here is based on the receiver model of Fig. 1 which shows the part of the receiver for a digital wireless system that is relevant to recovering the envelope of the signal. The white Gaussian noise $n(t)$ is added to the channel output. The result is passed through an ideal bandpass filter (BPF) centered at carrier frequency f_c with bandwidth $2/T$, where T is the symbol duration of the digitally modulated waveform. The signal is then passed through a square-law device followed by a unit-gain, square-root raised cosine lowpass filter (LPF) with bandwidth $2f_m(1+\gamma)/(1-\gamma)$. The maximum Doppler frequency at the highest speed of interest is f_m, and the excess bandwidth factor is γ ($0 < \gamma < 1$). The square root of the resulting signal is the envelope

Let the noise $n_{\mathrm{BPF}}(t)$ at the output of the bandpass filter be represented by in-phase and quadrature components: $n_{\mathrm{BPF}}(t) = n_I(t)\cos(2\pi f_c t) - n_Q(t)\sin(2\pi f_c t)$. The components $n_I(t)$ and $n_Q(t)$ each have variance σ_n^2. The curve Γ

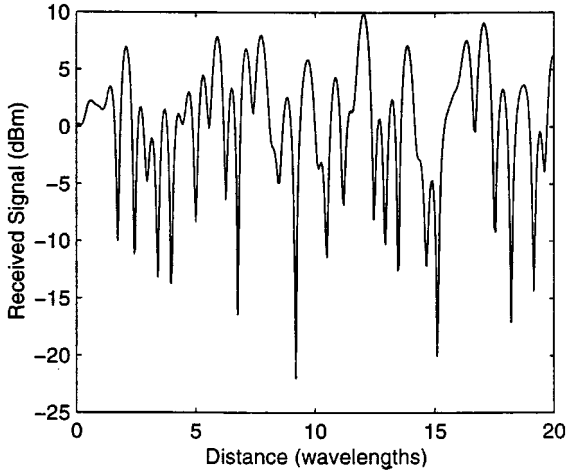

Fig. 2. Typical signal trace as a function of distance.

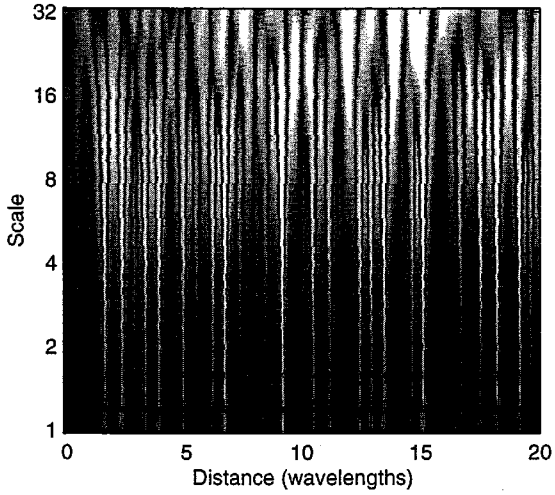

Fig. 3. Absolute value of CWT of signal given in Fig. 2. White represents large magnitude; black represents small magnitude.

traversed by the mobile station is parametrized by the scalar position variable $x(t)$. Suppose that the mobile travels along Γ with a speed $v(t)$ at time t. Under a narrow-band assumption, the square of the received envelope, $r^2(t)$, as a function of t is then

$$r^2(t) \approx |r_c(\Gamma[x(t)])|^2 + \text{LPF}\{n_I^2(t) + n_Q^2(t) + 2n_I(t)r_I(\Gamma[x(t)]) + 2n_Q(t)r_Q(\Gamma[x(t)])\} \quad (8)$$

where LPF denotes lowpass filtering with the square-root raised cosine filter and $x(t) = \int_0^t v(t')\,dt'$. The time origin is chosen such that $x(0) = 0$. We define $b_0 \equiv p(\boldsymbol{x}, \boldsymbol{x_B})$ and an input signal-to-noise ratio (SNR) as $\text{SNR}_i \equiv b_0/\sigma_n^2$. From the receiver model of Fig. 1, one can derive the average SNR at the output of the low-pass filter

$$\text{SNR}_o = \frac{(1-\gamma)\text{SNR}_i^2}{2f_m T(1+2\text{SNR}_i)}. \quad (9)$$

It is found that for the purpose of this paper, the cross terms in (8) can be ignored. Thus, the model for $r^2(t)$ simplifies to

$$r^2(t) \approx |r_c(\Gamma[x(t)])|^2 + \text{LPF}\,\{n_I^2(t) + n_Q^2(t)\}. \quad (10)$$

The logarithm of $r(t)$ is $f(t) \equiv 20\log_{10} r(t)$. The model presented here is used in Section III to estimate the mean signal.

III. Estimation of Mean Signal Using CWT

The estimation technique presented here utilizes the characteristic spatial scale of correlated Rayleigh fading. In the following, we consider the case of two-dimensional isotropic scattering such that the incoming power is uniformly distributed in azimuth angle θ and is given by $s(\theta) = 1/(2\pi), -\pi \le \theta < \pi$ [1]. Fig. 2 is a plot of a typical (noiseless) signal trace as a function of mobile position (measured in wavelengths). This plot shows that the local minima of the signal occur with an average separation of a fraction of a wavelength. The mean separation in distance between the local minima of the noiseless envelope is calculated in [8] to be approximately 0.662λ for the model stated above.

Let r_i^{mid} and $r_i^{\text{mid,nl}}$ denote signal samples taken at the midpoints between the local minima of the noisy and noiseless envelopes, respectively. Let the mean of $r_i^{\text{mid,nl}}$ be represented by $E\{r_i^{\text{mid,nl}}\} = \mu\sqrt{b_0}$ where μ is a constant determined in Section IV and $b_0 = b_0(t)$. An estimate of the mean signal is then

$$\widehat{\sqrt{b_0(t)}} = \frac{1}{\mu}\left(\text{local average}\left\{r_i^{\text{mid}}\right\}\right) \quad (11)$$

where the local average is taken in a neighborhood of time t. A method to estimate r_i^{mid} using the CWT is described in the following.

The CWT of a function $h(t) \in L_2(\mathcal{R})$ is given by

$$\text{CWT}_h(a,b) \equiv \frac{1}{\sqrt{a}}\int_{-\infty}^{\infty} \psi\left(\frac{t-b}{a}\right) h(t)\,dt \quad (12)$$

where $a \in \mathcal{R}^+$ denotes "scale" and $b \in \mathcal{R}$ denotes "shift." The "mother wavelet" $\psi(t) \in L_2(\mathcal{R})$ is a zero-mean, real function which satisfies the admissibility condition

$$C_\psi = \int_0^\infty \frac{|\Psi(\omega)|^2}{|\omega|}\,d\omega = \int_{-\infty}^0 \frac{|\Psi(\omega)|^2}{|\omega|}\,d\omega < \infty \quad (13)$$

where $\Psi(\omega)$ is the Fourier transform of $\psi(t)$. Fig. 3 is a plot of the absolute value of a CWT of the signal given in Fig. 2.

The CWT has the important property of characterizing singularities of the signal [9]–[11]. Since many of the local minima of $f(t)$ correspond to points of discontinuity in the first derivative, the CWT is used to detect the local minima.[1] Detecting the local minima using the CWT permits the tracking of a variable mobile speed profile without requiring an adaptive window. In contrast, other function minimization methods using a three-point bracketing scheme require adaptation of the bracketing time since the time between local minima varies as the speed varies.

As discussed in detail in Section IV-D, the CWT of $f(t)$ is taken over a suitable temporal window of observation to obtain

[1]The local minima of the envelope $r(t)$ correspond to the local minima of the logarithm of the envelope $f(t)$. The noiseless version of $f(t)$ is related to the signal of Fig. 2 through the mobile speed $v(t)$.

mean signal estimates within an acceptable delay for real-time implementation. The CWT is taken at a discrete set of scales $a = 2^{l+m/M}, l = l_{\min}, l_{\min}+1, \ldots, l_{\max}, m = 0, \ldots, M-1$, where $l_{\min}$, $l_{\max}$, and M are integers. In order to compare the CWT to a significance threshold which is independent of mobile speed, the CWT of $f(t)$ at each scale a is normalized by $1/\sqrt{a}$ before further processing.

One method to detect the points of discontinuity in the first derivative of $f(t)$ is to identify the wavelet transform modulus maxima [10] (WTMM). The number of WTMM associated with a singularity of $f(t)$ depends upon the number of local extrema of the analyzing wavelet $\psi(t)$. The number of local extrema of the wavelet is at least one plus the number of vanishing moments of the wavelet. Furthermore, the analyzing wavelet must have at least two vanishing moments in order to characterize points of $f(t)$ which have discontinuous derivatives.

The singularities of interest for mean signal estimation are the points with discontinuous derivative that are also local minima of $f(t)$. This fact can be used to reduce the number of extraneous WTMM by using a modified version of the WTMM detection method as described in the following. For wavelets $\psi(t)$ which satisfy $\sup_t \psi(t) \geq -\inf_t \psi(t)$, the *negative local minima* at each scale of the normalized CWT are identified; otherwise, the *positive local maxima* at each scale are identified. The values identified as above are referred to as the *signed local extrema* of the normalized CWT. The benefit of using the signed local extrema instead of the modulus maxima is that for a suitable analyzing wavelet $\psi(t)$, the local minima of $f(t)$ with discontinuous derivative do not produce extraneous signed local extrema. In contrast, each singularity of $f(t)$ gives rise to extraneous modulus maxima using the WTMM method. Therefore, use of the signed local extrema removes the need to isolate the modulus maxima from the extraneous ones. The signed local extrema with absolute value less than a significance threshold τ are discarded. The scale which has the highest number of significant signed local extrema is identified as the scale of interest and is denoted by a_τ.

Since most of the local minima of $f(t)$ correspond to points of discontinuity in the first derivative, the locations in time of the signed local extrema of the normalized CWT correspond to most of the locations of the local minima of $f(t)$ (and, hence, the local minima of $r(t) = 10^{f(t)/20}$). To compensate for the small fraction of local minima of $f(t)$ with continuous derivative, the significance threshold τ is determined empirically such that the number of local minima of $f(t)$ which are detected by the CWT is equal to the total number of local minima of $f(t)$. The selection of τ is discussed in more detail in Section IV-B.

We now consider $(N+1)$ significant signed local extrema occurring at times $t_0, t_1, \ldots, t_N$. The mean of the signal at the midpoints between the local minima of $r(t)$ is estimated by the signal samples taken at the midpoints between the signed local extrema of the CWT, i.e., $\hat{r}_i^{\text{mid}} = r(\tilde{t}_i), i = 0, 1, \ldots, N-1$, where $\tilde{t}_i = (t_i + t_{i+1})/2$. The estimate (11) for $\sqrt{b_0(t)}$ at time $(\tilde{t}_0 + \tilde{t}_{N-1})/2$ then becomes

$$\widehat{\sqrt{b_0((\tilde{t}_0 + \tilde{t}_{N-1})/2)}} = \frac{1}{N\mu} \sum_{i=0}^{N-1} \hat{r}_i^{\text{mid}}. \tag{14}$$

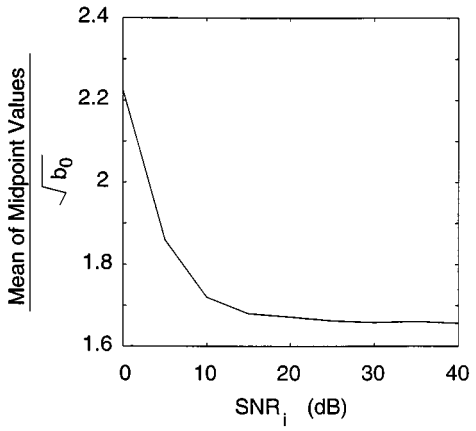

Fig. 4. Mean of midpoint values versus input signal-to-noise ratio (SNR$_i$).

The next estimate of the mean signal is $\widehat{\sqrt{b_0((\tilde{t}_1 + \tilde{t}_N)/2)}}$, which is obtained by considering a time interval containing a new signed local extremum and the N most recent signed local extrema from the previous time interval. The estimates obtained in this manner are linearly interpolated to the signal sampling rate. The resulting signal is smoothed by a moving average. The following section describes the selection of parameters together with simulations which apply the estimation technique.

IV. Parameter Selection and Simulation Results

This section determines the mean of the signal samples taken at midpoints between local minima of the received envelope and selects the significance threshold (τ) and the number (N) of midpoint values used. The choice of the maximum scale ($a_{\max}$), the duration (T_{obs}) of the observation window over which the CWT is taken, and associated boundary effects are also described. The observation window is required to obtain estimates within an acceptable delay for real-time implementation. The performance of the mean signal estimator is then compared to the adaptive averaging method described in [5] for constant and variable mobile speed.

A. Mean of Signal Samples Taken at Midpoints Between Local Minima

The mean of the signal samples taken at the midpoints between the local minima is determined by averaging over 90 independent realizations of the Rayleigh fading process with constant b_0 and with around 1000 local minima per realization. The resulting value is $E\{r_i^{\text{mid,nl}}\} = \mu\sqrt{b_0} \approx 1.66\sqrt{b_0}$. The effect of noise on this mean value is also investigated. Fig. 4 is a plot of the mean of the midpoint values normalized by $\sqrt{b_0}$ as a function of SNR$_i$. Each point represents an average over ten independent realizations of the Rayleigh fading and noise processes. The excess bandwidth of the square-root raised cosine low-pass filter of Fig. 1 is chosen to be $\gamma = 0.5$. The mean signal power b_0 and the noise variance σ_n^2 are kept constant for each value of SNR$_i$ to obtain results under a controlled environment. For SNR$_i$ $>$ 15 dB, the mean of the midpoint values approaches the noiseless value of $1.66\sqrt{b_0}$.

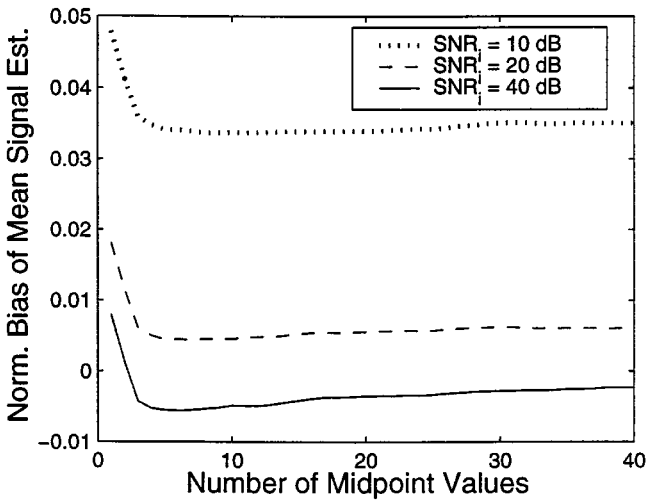

Fig. 5. Normalized bias versus number of midpoint values.

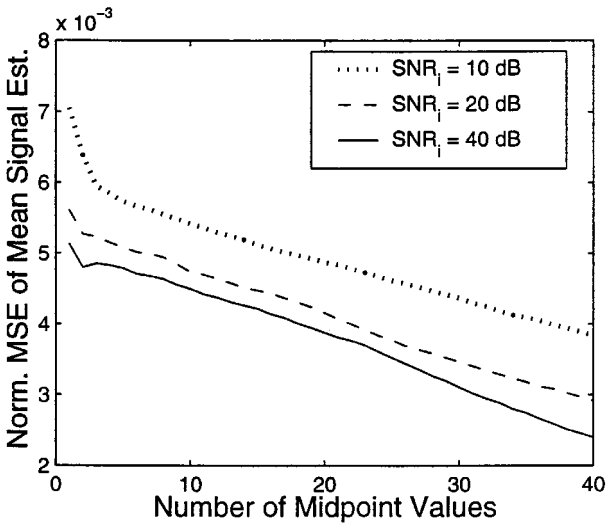

Fig. 6. Normalized MSE versus number of midpoint values.

B. Selection of Significance Threshold

The threshold τ is selected such that the number of signed local extrema that are detected at scale a_τ is equal to the number of positive-slope zero crossings of the derivative $f'(t)$ in the absence of noise. The threshold τ depends on the analyzing wavelet $\psi(t)$. The wavelet chosen is a "coiflet" of order 2 (coif1) [9]. This wavelet has two vanishing moments and yielded the best results among the five different wavelets considered in [8]. The optimum threshold of $\tau = 0.474$ for the coif1 wavelet was determined by averaging over 90 independent realizations of the Rayleigh fading process.

C. Number of Midpoint Values

Fig. 5 is a plot of the normalized bias of the mean signal estimate, $E[(\widehat{\sqrt{b_0}}/\sqrt{b_0}) - 1]$, as a function of the number (N) of midpoint samples for various values of SNR$_i$. The mean signal power b_0 and noise variance σ_n^2 are kept constant for each value of SNR$_i$ to obtain results under a controlled environment. The results are obtained by averaging over ten independent realizations of the Rayleigh fading process for each value of SNR$_i$; the received envelope for each realization has approximately 1000 local minima. The bias is found to be negligible for $N > 4$ and SNR$_i > 15$ dB. The normalized mean square error (MSE) of the mean signal estimate, $E\{[(\widehat{\sqrt{b_0}}/\sqrt{b_0}) - 1]^2\}$, as a function of N is plotted in Fig. 6. For the range of N shown in Fig. 6, the MSE varies almost linearly with N since, for small N, the MSE is dominated by the moving average of the mean signal estimates. For larger N, the MSE decreases as $1/N$.

D. Maximum Scale, Duration of Observation Window, and Boundary Effects

The CWT is applied to blocks of the signal collected over time periods of duration $T_{\rm obs}$ in order to limit the delay in obtaining mean signal estimates for real-time implementation. The determination of $T_{\rm obs}$ is described in the following. Let the lowest speed of interest be denoted by $v_{\min}$, i.e., speeds less than $v_{\min}$ will be regarded as zero. If L_ψ denotes the nominal duration of support of the analyzing wavelet $\psi(t)$, the maximum scale for the CWT is $a_{\max} = 0.662\lambda/(L_\psi v_{\min})$. The duration of the observation window is then the mean time between local minima of the signal for a mobile speed of $v_{\min}$, i.e., $T_{\rm obs} = 0.662\lambda/v_{\min}$. The finite observation window results in boundary effects in the detection of the signed local extrema of the CWT. In order to remove these effects, the observation windows are enlarged by $T_{\rm obs}/2$ for each boundary (left and right endpoints). The enlarged windows slide by an amount $T_{\rm obs}$ as time progresses. For the initial left boundary and the final right boundary, the signal $f(t)$ is reflected about the boundaries such that $f(t)$ and the first derivative $f'(t)$ are continuous at the boundaries. This technique of overlapping windows results in a factor of two increase in computation for the CWT and a $T_{\rm obs}/2$ increase in delay of the mean signal estimate.

E. Comparison to Adaptive Averaging Method

The mean signal estimator presented here is compared to the adaptive averaging method described in [5]. The adaptive averaging technique uses the squared deviations of $f(t)$ to estimate the maximum Doppler frequency f_m. The estimate of f_m is used to determine the number of samples of $f(t)$ which are averaged to estimate $10\log_{10} b_0(t)$. In Fig. 7, the normalized bias of the two methods is compared for a constant mobile speed. As in Section IV-C, the results are obtained by averaging over ten independent realizations of the Rayleigh fading process for each value of SNR$_i$; the received envelope for each realization has approximately 1000 local minima. The spatial averaging distance for both methods is 20λ, in accordance with the results given in [3]. The spatial averaging distance of 20λ implies that the number of midpoint values used in (14) is $N = 20/0.662 \approx 30$. For the adaptive averaging method, the number of samples of $f(t)$ corresponding to 20λ depends on the current estimate of f_m. Fig. 8 is a plot of the normalized MSE of the two estimation methods. It can be seen that the mean signal estimator using wavelets performs better over a large range of SNR$_i$.

F. Variable Mobile Speed Example

The performance improvement of the wavelet method over the adaptive averaging method is vivid for a variable mobile

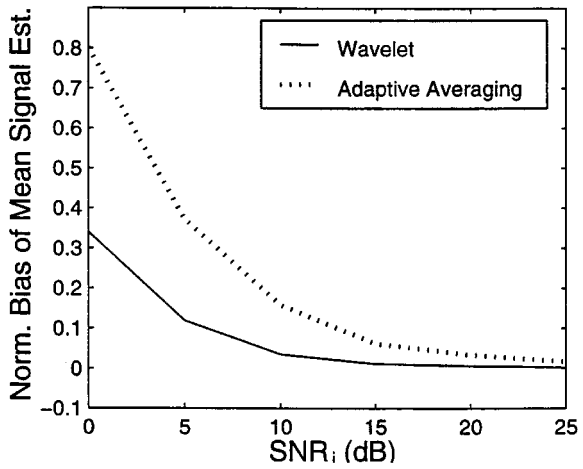

Fig. 7. Normalized bias versus SNR$_i$ for wavelet and adaptive averaging methods.

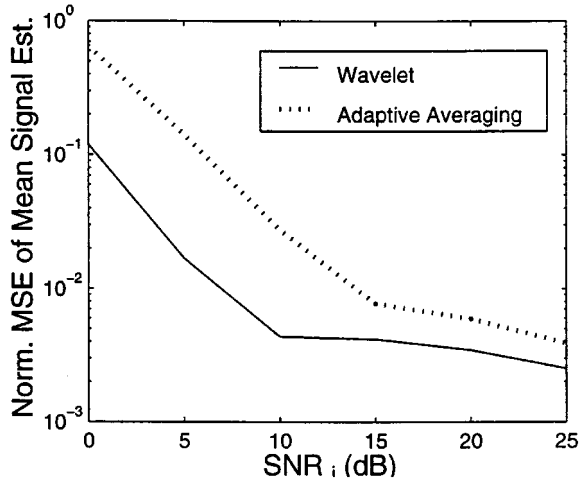

Fig. 8. Normalized MSE versus SNR$_i$ for wavelet and adaptive averaging methods.

speed profile. The performances of the two estimators are compared using the following mobile speed profile $v(t)$ (in km/h):

$$v(t) = \begin{cases} 0 & 0 \le t < 0.5 \\ 100\,\xi\left(\dfrac{t-0.5}{8}\right) & 0.5 \le t < 8.5 \\ 100 & 8.5 \le t < 11.5 \\ 100\,\xi\left(\dfrac{19.5-t}{8}\right) & 11.5 \le t < 19.5 \\ 0 & 19.5 \le t \le 20 \end{cases} \tag{15}$$

where

$$\xi(t) = \begin{cases} 0 & t < 0 \\ 3t^2 - 2t^3 & 0 \le t < 1 \\ 1 & 1 \le t. \end{cases} \tag{16}$$

Fig. 9 is a plot of the logarithm of the noiseless envelope and the mean signal power in decibel, $10\log_{10} b_0(t)$, for the speed profile given in (15). The duration of the moving average for smoothing of the estimates obtained in (14) is chosen to be $T_{\rm obs}$. The relevant parameters for this example are summarized in Table I.

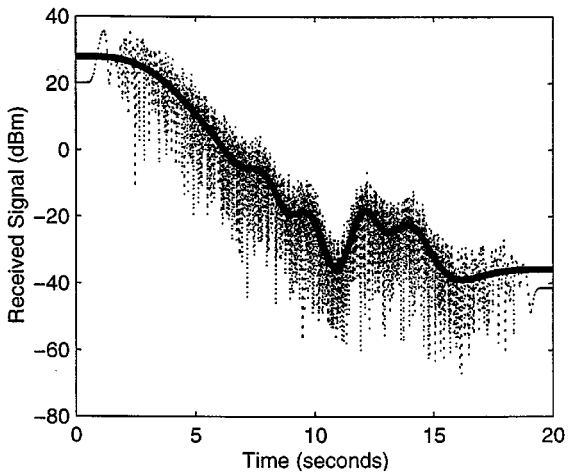

Fig. 9. Logarithm of noiseless envelope (dotted) and mean signal power in decibel (solid) for speed profile given in (15).

TABLE I
PARAMETERS FOR VARIABLE SPEED EXAMPLE

Parameter	Description	Value
$\psi(t)$	Analyzing Wavelet	coiflet, order 2
M	Number of Scales per Octave	6
λ	Wavelength	1/3 m
α	Path Loss Exponent	4
$\sigma_L(\mathbf{x_B})$	Shadowing Standard Deviation	10 dB
$d_0(\mathbf{x_B})$	Shadowing Correlation Length	50 m
K	Terms in Fading Model	100
N	Number of Midpoint Values	30
$v_{\min}$	Minimum Speed	1.8 km/h
$T_{\rm obs}$	Observation Window	0.44 s

Fig. 10 is a plot of the error (in decibels) between the estimate and the true mean signal power for the two estimation methods and for the speed profile given in (15). A value of 0 dB for the ordinate in Fig. 10 implies no estimation error. An estimation error less than 0 dB implies an underestimate while an error greater than 0 dB implies an overestimate. A mobile speed of zero at the left and right endpoints of Fig. 10 contributes to estimation errors at either or both endpoints. At very low mobile speeds, any method to estimate the mean signal may have significant estimation errors since a sufficient number of samples of the Rayleigh fading process is not available within a given time interval to obtain accurate estimates. An advantage of the wavelet method is that the method can detect the presence of local minima in the signal. If no minima are detected, one concludes that the mobile speed is very low (less than $v_{\min}$), and hence no system action (e.g., handoff or channel assignment) need be taken. Fig. 10 shows that the mean signal estimator using wavelets performs significantly better than the adaptive averaging method for variable mobile speed.

V. CONCLUSION

The paper presents a new technique for estimating the mean signal in a Rayleigh fading environment. A wireless propagation model is used which accounts for correlated Rayleigh fading, correlated log-normal shadowing, and a distance-dependent trend. A noise model is also described which takes into consideration the signal processing required to obtain the

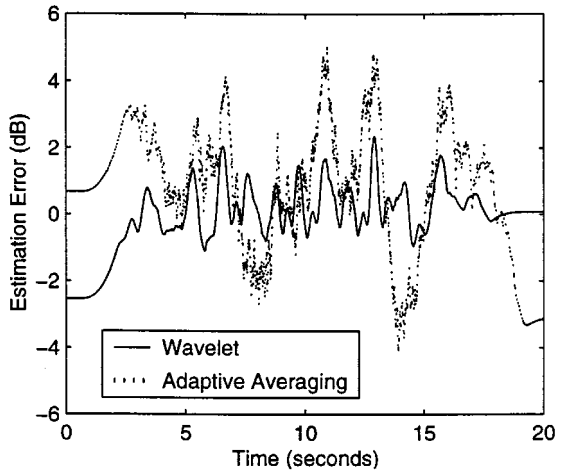

Fig. 10. Estimation error for wavelet method and adaptive averaging method using speed profile given in (15).

received envelope. The mean signal is estimated by computing a local average of the signal samples taken at the midpoints between adjacent local minima of the received envelope. With an empirically determined significance threshold, the significant signed local extrema of the CWT are used to detect the local minima. This estimation technique is robust under variable mobile speeds and performs better than an adaptive averaging method described in the literature.

REFERENCES

[1] W. C. Jakes, *Microwave Mobile Communications*. New York: Wiley, 1974.

[2] A. J. Goldsmith, L. J. Greenstein, and G. J. Foschini, "Error statistics of real-time power measurements in cellular channels with multipath and shadowing," *IEEE Trans. Veh. Technol.*, vol. 43, pp. 439–446, 1994.

[3] W. C. Y. Lee, "Estimate of local average power of a mobile radio signal," *IEEE Trans. Veh. Technol.*, vol. VT-34, pp. 22–27, 1985.

[4] D. Wong and D. C. Cox, "An optimal local mean signal power level estimator for Rayleigh fading environments," in *Proc. Int. Conf. Info., Comm., Signal Proc.*, 1997, pp. 1701–1704.

[5] J. M. Holtzman and A. Sampath, "Adaptive averaging methodology for handoffs in cellular systems," *IEEE Trans. Veh. Technol.*, vol. 44, pp. 59–66, 1995.

[6] D. C. Cox, "Universal digital portable radio communication," *Proc. IEEE*, vol. 75, pp. 436–477, 1987.

[7] M. Gudmundson, "Correlation models for shadow fading in mobile radio systems," *Electron. Lett.*, vol. 27, no. 23, pp. 2145–2146, 1991.

[8] R. Narasimhan and D. C. Cox, "Speed estimation in wireless systems using wavelets," *IEEE Trans. Commun.*, vol. 47, pp. 1357–1364, Sept. 1999.

[9] I. Daubechies, "Ten lectures on wavelets," in *CBMS-NSF Series Appl. Math.*: SIAM, 1992.

[10] S. Mallat and W. L. Hwang, "Singularity detection and processing with wavelets," *IEEE Trans. Inform. Theory*, vol. 38, pp. 617–643, 1992.

[11] M. Vetterli and J. Kovačević, *Wavelets and Subband Coding*. Englewood Cliffs, NJ: Prentice-Hall, 1995.

Ravi Narasimhan (S'96–M'99) received the B.S. degree (with highest honors) in electrical engineering, the Certificate of Distinction from the University of California at Berkeley in 1995, and the M.S. and Ph.D. degrees in electrical engineering from Stanford University in 1996 and 2000, respectively. He is presently at Marvell Semiconductor, Inc., Sunnyvale, CA.

Dr. Narasimhan is a member of Phi Beta Kappa and Golden Key National Honor Society. He received the Warren Y. Dere Memorial Prize from University of California at Berkeley in 1995. He secured the first rank in the Ph.D. qualifying examination in electrical engineering at Stanford University. He also received the Best Student Paper Award for U.S. at the IEEE International Symposium on Personal, Indoor and Mobile Radio Communications (PIMRC), held in Boston, MA, September 1998. His research interests include wireless communication, signal processing, and wavelet analysis.

Donald C. Cox (S'58–M'61–SM'72–F'79) received the B.S. and M.S. degrees in electrical engineering from the University of Nebraska, Lincoln, in 1959 and 1960, respectively, and the Ph.D. degree in electrical engineering from Stanford University, Stanford, CA, in 1968. He received an Honorary Doctor of Science from the University of Nebraska in 1983.

From 1960 to 1963, he did microwave communications system design at Wright-Patterson AFB, OH. From 1963 to 1968, he was at Stanford University doing tunnel diode amplifier design and research on microwave propagation in the troposphere. From 1968 to 1973, his capacity mobile radio systems provided important input to early cellular mobile radio system development, and is continuing to contribute to the evolution of digital cellular radio, wireless personal communications systems and cordless telephones. From 1973 to 1983, he was Supervisor of a group at Bell Laboratories that did innovative propagation and system research for millimeter-wave satellite communications. In 1978, he pioneered radio system and propagation research for low-power wireless personal communications systems. At Bell Laboratories in 1983 he organized and became Head of the Radio and Satellite Systems Research Department that became a Division in Bell Communications Research (Bellcore) with the breakup of the Bell System on January 1, 1984. He was Division Manager of that Radio Research Division until it again became a department in 1991. He continued as Executive Director of the Radio Research Department where he championed, led and contributed to research on all aspects of low-power wireless personal communications entitled Universal Digital Portable Communications (UDPC). He was instrumental in evolving the extensive research results into specifications that became the U.S. Standard for the Wireless or Personal Access Communications System (WACS or PACS). In September 1993, he became a Professor of Electrical Engineering and Director of the Center for Telecommunications at Stanford University where he continues to pursue research and teaching of wireless mobile and personal communications. He was appointed Harald Trap Friis Professor of Engineering in 1994. He is author or coauthor of many papers and conference presentations, including many invited and several keynote addresses, and books. He has been granted 15 patents.

Dr. Cox was a member of the Administrative Committee of the IEEE Antennas and Propagation Society (1968–1988), was an Associate Editor of the IEEE TRANSACTIONS ON ANTENNAS AND PROPAGATION (1983–1986), is a member of the National Academy of Engineering, is a member of Commissions B, C, and F of USNC/URSI, and was a member of the URSI Intercommission Group on Time Domain Waveform Measurements (1982–1984). He was awarded the IEEE 1993 Alexander Grapham Bell Medal "For pioneering and leadership in personal protable communications"; was a co-recipient of the 1983 International Marconi Prize in Electromagnetic Wave Propagation (Italy); received the IEEE 1985 Morris E. Leeds award and the IEEE Third Millennium Medal in 2000; and received the 1983 IEEE Vehicular Technology Society paper of the year award, and the IEEE Communications Society 1992 L. G. Abraham Prize Paper Award and 1990 Communications Magazine Prize Paper Award. He received the Bellcore Fellow Award in 1991. He is a fellow of AAAS and the Radio Club of America. He is a member of Sigma Xi, Sigma Tau, Eta Kappa Nu and Phi Mu Epsilon, and is a Registered Professional Engineer in Ohio and Nebraska.